



The different catalytic effects of Na species on char gasification and the reasons for this different

Li Li^{1,2} · Zhiqing Wang¹ · Rong Zhao¹ · Yangang Mei^{1,2} · Wenju Shi^{1,2} · Zheyu Liu¹ · Jiejie Huang¹ · Yitian Fang¹

Received: 1 March 2020 / Accepted: 4 May 2021 / Published online: 26 June 2021
© Akadémiai Kiadó, Budapest, Hungary 2021

Abstract

To study the effect of anion in sodium salts on catalytic gasification and provide some useful information for the recovery and reutilization of catalysts, the catalytic reactivity of Na_2CO_3 , Na_2SO_4 , NaNO_3 and NaCl was compared. In addition, the melting process of catalyst, mineral composition, specific surface area and CO_2 adsorption ability of chars loaded with catalyst was measured by in situ hot stage microscope, XRD, BET and TGA. Moreover, the mineral transformations of catalytic gasification ash were also investigated by FactSage. The results indicate that anions in sodium salts have a significant effect on gasification. Among them, Na_2SO_4 and Na_2CO_3 can greatly accelerate the catalytic gasification rate of coal char. The char loaded with Na_2SO_4 or Na_2CO_3 shows more specific surface area and more adsorption capacity of CO_2 than other chars. Simultaneously, the pictures captured by hot stage microscope reveal that Na_2SO_4 and Na_2CO_3 melt, become liquid film and then spread over char surface and neighboring particles; this facilitates the contact between carbon and catalyst and accelerates the gasification reaction. Na_2SO_4 is suitable for catalytic gasification from the aspects of its catalytic activity and convenience of recovery and reutilization.

Keywords Coal char · Catalytic gasification · Na species · Catalyst recovery and reutilization

Introduction

Gasification is an efficient technology that can convert carbonaceous materials such as coal [1], biomass [2, 3], household garbage [4, 5] into small molecules (H_2 , CO , CH_4 , etc.). It is also considered as a promising technology to realize clean utilization of some contaminative carbonaceous fuels [1, 6]. After gasification, the contamination in the impure fuels can be converted to harmless matters or gas during gasification. More importantly, the H_2 and CO in gasification product are commonly raw chemical material that can be used to produce methanol [7], dimethyl ether [8], ammonia, etc. These products play an important role in our daily production and directly related to the quality of our life.

Generally, to obtain a faster reaction rate and higher carbon conversion, coal is gasified with gasification agent (steam, air, O_2 or CO_2) at high temperatures (1573.15–2073.15 K) and high pressures (0.5–8.0 MPa) [9], especially for coal with poor gasification reactivity. These rigorous conditions lead to high energy consumption and increase operational risk [10]. Catalytic gasification can partially solve the above-mentioned problem by speeding up the reaction rate and decreasing the reaction temperature significantly [11–14]. Alkali and alkali earth metal salts [12, 15–19], nickel [20] and iron compounds [21] are considered as effective catalysts. Among them, alkali metal carbonate has the best performance and thus has roused scholars' particular interest [22–25]. Jan Kopyscinski et. al. [26] chose K_2CO_3 as the catalyst and found that the gasification rate was 20 times faster than that of non-catalytic gasification. Arash Karimi et. al. [25] found that the activation energy of gasification reaction reduced from $2.1 \times 10^5 \text{ J mol}^{-1}$ to $1.3 \times 10^5 \text{ J mol}^{-1}$ by the addition of Na_2CO_3 . Fan Zhang et. al. [27] found that 29.7% of activation energy reduction was realized by the addition of Na_2CO_3 . Our previous study [28] has shown that Na_2CO_3 has better catalytic activity than K_2CO_3 in the steam gasification while its price is about

✉ Zhiqing Wang
qcumt@sxicc.ac.cn

¹ State Key Laboratory of Coal Conversion, Institute of Coal Chemistry, Chinese Academy of Sciences, Taiyuan, Shanxi 030001, People's Republic of China

² University of Chinese Academy of Sciences, Beijing 100049, People's Republic of China

one-quarter of K_2CO_3 , so Na_2CO_3 is a promising catalyst for industrial application.

However, industrialization of catalytic gasification in large-scale has not been achieved so far. One of the issues is the recovery and reutilization of catalyst, for the catalyst used in gasification can react with minerals in coal inevitably and form inactive water-insoluble Na-containing compounds [29–31]. This water-insoluble property decides Na-containing compounds cannot be recovered by water. Thus, the acid-leached method is generally used. At the same time, acid leaching can also extract compounds containing Al or Si from the gasification ash, so that the useful substances in the ash can be effectively utilized. However, in the acid-leached process, the type of acid used in the acid-leached process determines the recovery type of alkali salt, while the recovery type of alkali salt usually affects its reutilization. For example, HCl, which acts as an extracting agent, is usually used for extracting compounds containing Al from ash which has been activated. If HCl were selected, the recovery type of sodium salt would be NaCl (no matter which kind of Na species was used as catalyst). Unfortunately, the catalytic activity of NaCl is poor and NaCl is no longer suitable as catalyst (as shown in this study), which results in this recovery method insignificant. Thus, the recovery method must adapt himself for the catalytic activity of recovered sodium salt, this urgent problem, so to speak, must be solved before a large-scale and workable gasification technology is applied.

H_2SO_4 , H_2CO_3 , HNO_3 and HCl are frequently used acids in the acid-leached process, their anions are CO_3^{2-} , SO_4^{2-} , NO_3^- and Cl^- , and the corresponding recovered sodium salts are Na_2CO_3 , Na_2SO_4 , $NaNO_3$ and NaCl. Thus, the catalytic activity of these recovered sodium salts, their catalytic processes, the effect of anions on catalytic gasification and the inactivation behaviors induced by minerals during gasification must be evaluated before a suitable recovery method is selected. Unfortunately, even many scholars [29] have done researches on gasification catalysts; previous works did not separately consider the effect of anions on catalytic

gasification, did not systematically and comparatively studied the above-mentioned problems and thus cannot provide direct guidance for the choice of suitable acid in the catalyst recovery process.

In this study, the catalytic effects of Na species (Na_2CO_3 , Na_2SO_4 , $NaNO_3$, NaCl) on coal char gasification reactivity were investigated. Then, in order to find out the reasons for the difference in catalytic activity, hot stage microscope (visually observe and record the gasification processes), BET (specific surface area and pore distribution), the CO_2 adsorption capacity (the active sites of catalyst loaded char, reflect the effect of a catalyst on gasification reaction), XRD and thermodynamic equilibrium calculations of the mineral and sodium salts (FactSage, the inactivation behaviors induced by minerals) were investigated. The objectives of this study are (1) to explore the reasons of accelerating the gasification reaction rate and carbon conversion by adding sodium salt catalysts and (2) to compare the catalytic gasification reactivity of sodium salts with different anions on the basis of equal mole mass and provide useful information on the process of catalysts recovery and reutilization. The realization of these two objectives is the prerequisite for industrial catalytic gasification and extraction of compounds containing Al or Si in coal ash.

Experimental

Samples and reagents

The raw coal from Inner Mongolia was ground and sieved to less than $125\ \mu\text{m}$. Then, it was dried in oven and collected in desiccator as coal sample. The proximate and ultimate analyses of the coal sample are listed in Table 1, and the ash composition is presented in Table 2, Fig. 1. All the chemical reagents, which include Na_2CO_3 , Na_2SO_4 , $NaNO_3$ and NaCl, were purchased from Sinopharm Chemical Reagent Co., and their purity was above 99%.

Table 1 Proximate and ultimate analyses of coal sample

Proximate analysis/mass %, ad ^a				Ultimate analysis /mass %, daf ^b				
M	A	V	FC	C	H	O ^c	N	S
0.80	27.77	20.70	50.73	86.42	5.29	4.05	1.48	2.76

^aad = air-dried basis.

^bdaf = dry and ash-free basis

^cby difference

Table 2 Ash compositions (mass %) of coal sample

SiO ₂	Al ₂ O ₃	Fe ₂ O ₃	CaO	MgO	TiO ₂	SO ₃	K ₂ O	Na ₂ O	P ₂ O ₅
50.11	38.33	6.30	0.61	0.42	0.84	0.36	0.85	0.16	0.07

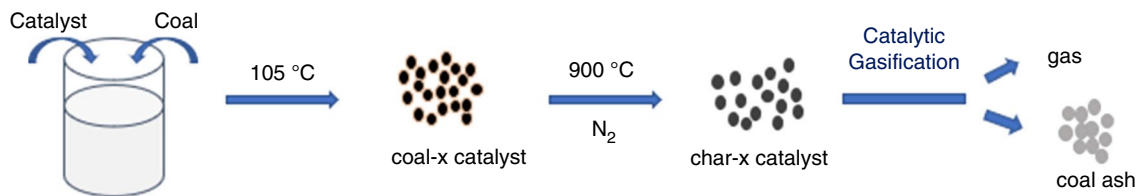


Fig. 1 Diagram of experimental steps

Catalyst loading and coal char preparation

Impregnation method was used and the addition of catalysts obeyed the following rule: Per unit mass of coal correspond to a certain mole of Na⁺ in solution. Detailed preparation processes were similar to our previous work [16]. Firstly, 0.15 mol of Na₂CO₃ was dissolved in 200 mL of deionized water. Then, 0.1 kg of coal sample was added in it with continuous stirring until the coal sample was completely mixed with the solution. After that, this mixed slurry was dried in oven and ground to less than 125 μm. This sample (per kilogram of coal that had been loaded with 1.5 mol of Na₂CO₃) was called coal-1.5 Na₂CO₃. Similarly, other coal samples which were loaded with catalysts (Na₂SO₄, NaNO₃ or NaCl) by the rule (per kilogram of coal corresponds to x mole of catalyst) were called coal-x Na₂SO₄, coal-x NaNO₃ or coal-x NaCl, respectively.

Coal char was prepared by pyrolyzing coal in the N₂ atmosphere at high temperature. Detailed steps were as below: spread 10 g of coal-1.5 Na₂CO₃ in an alumina boat evenly and then pushed the boat to the isothermal zone of the tubular. At the same time, N₂ with 200 mL min⁻¹ flowed through the tubular furnace. 20 min later, the furnace was heated with a rate of 5 K min⁻¹ to 1173.15 K and stabilized for 20 min to pyrolyze coal-1.5 Na₂CO₃. Then, the furnace was cooled under the N₂ atmosphere and the alumina boat could be removed when the temperature dropped to below 373.15 K. This char sample was called char-1.5 Na₂CO₃. Similarly, other coal samples such as coal-Na₂SO₄, coal-NaNO₃ and coal-NaCl pyrolyzed with this method were called char-Na₂SO₄, char-NaNO₃ and char-NaCl, respectively.

CO₂ gasification of coal char in TGA

Coal char gasification was conducted by a Setaram SETSYS thermogravimetric analyzer (TGA). About 7 mg of char sample was evenly spread in a crucible. Then, it was heated with a rate of 20 K min⁻¹ to target temperature (1073.15–1223.15 K) in N₂ (99.9%, 100 mL min⁻¹) and maintained for 20 min to stabilize the system. After that, N₂ was switched to CO₂ (99.8%, 100 mL min⁻¹) and the gasification began. When the mass curve became horizontal and basically no fluctuation, the gasification was finished.

Carbon conversion (x) was calculated as below: (where the added catalyst is regarded as a part of ash in coal and assumes that the mass of catalyst remains constant)

$$x = \frac{m_0 - m_t}{m_0 - m_c} \quad (1)$$

$$m_c = \frac{m_A + m_F}{1 + m_F} \times m_{\text{coal-catalyst}} \quad (2)$$

$$m_{\text{coal-catalyst}} = J \times m_0 \quad (3)$$

where m_0 represents the initial mass of char sample, m_t represents the mass of char sample at the time when gasification reaction lasted t min; m_c represents the mass of theoretical calculation value of char sample when the carbon was fully reacted in the gasification process; m_A represents the ash mass of per gram coal; m_F represents the added catalytic mass of per gram coal; $m_{\text{coal-catalyst}}$ represents the mass of coal loaded with catalyst; and J is a constant value (determined by experiment) and represents mass change of coal-x catalyst to char-x catalyst.

Gasification rate (r_t , min⁻¹) was calculated as below:

$$r_t = \frac{dx_t}{dt} = -\frac{1}{m_0 - m_c} \frac{dm}{dt} \quad (4)$$

The reactivity index ($R_{0.5}$) was a parameter to compare the gasification reactivity of various catalysts with different additions. $R_{0.5}$ was defined as below:

$$R_{0.5} = 0.5/\tau_{0.5} \quad (5)$$

$\tau_{0.5}$ was the time when the carbon conversion rate was 0.5.

CO₂ gasification of coal char in hot stage microscope

To in situ visually capture and record the gasification process at a relatively high temperature, the hot stage microscope was employed. About 1 mg of coal char was firstly placed on the center of the sapphire lens and then adjusted the focal length. After that, the hot stage microscope was heated with a rate of 50 K min⁻¹ to 1173.15 K in N₂ (99.9%, 50 mL min⁻¹). When the temperature reached 1173.15 K, N₂

was switched to CO₂ (99.8%, 50 mL min⁻¹) and the gasification began. Some morphology changes of coal char and catalyst appeared in this process.

Thermodynamic equilibrium calculations

Thermodynamic equilibrium calculations can provide the data of mineral content in catalytic gasification ash with different catalysts addition. The Equilib module in FactSage 6.4 with the FactPS and FToxid databases was used to calculate the concentration of chemical species under atmospheric pressure [32]. The input data include carbon in coal, ash compositions (Table 2), CO₂ and catalysts.

CO₂ adsorption of coal char

TGA was employed to test the CO₂ adsorption capacity of coal char. 15 mg of char was well placed in a crucible with N₂ (99.9%, 50 mL min⁻¹) flow. It was heated with a rate of 20 K min⁻¹ to 1173.15 K and maintained 10 min to remove the adsorbed gas in char. Then, it was cooled with a rate of 20 K min⁻¹ to 573.15 K and continued 30 min to stabilize the system. After that, N₂ was switched to CO₂ (99.8%, 50 mL min⁻¹) and lasted 100 min to adsorb CO₂ fully. Next, CO₂ was switched to N₂ again and sustained 150 min to remove the CO₂ that adsorbed on the coal char weakly. Finally, the temperature was cooled to 303.15 K with a rate of 20 K min⁻¹. All of the above experiments were repeated at least once.

Characterization methods

The proximate and ultimate analyses were conducted according to Chinese National Standards GB/T 212–2008 and GB/T 476–2001, respectively. Specific surface area and pore structure of coal char were measured with BET by N₂ adsorption and desorption at 77.15 K. The specific surface area was calculated by the BET model, and the pore size distribution was obtained by the BJH model. The crystal structures of catalytic gasification ash added with different kinds of catalysts were characterized by an X-ray diffractometer (D8 Advance, Bruker, Germany) using Cu K α radiation ($\lambda = 1.54056 \text{ \AA}$), a 30 kV tube voltage, a 15 mA tube current and a scan rate of 2° min⁻¹. The morphology of coal samples was obtained by a scanning electron microscope (SEM, JSM-7001F, JEOL, Japan).

Results and discussion

Catalytic gasification performance of char loaded with several Na⁺ contained catalysts

Na₂CO₃, Na₂SO₄, NaNO₃ and NaCl were used to investigate the catalytic effect of Na⁺ contained catalysts, systematically. The gasification behaviors of Char-1.5 Na₂CO₃, char-1.5 Na₂SO₄, char-3.0 NaNO₃ and char-3.0 NaCl are shown in Fig. 2. It reveals that all of the catalysts show catalytic activity and the order of it is as follows: Na₂SO₄ > Na₂CO₃ > NaNO₃ > NaCl. It obviously revealed that oxygen-containing sodium salts show better catalytic activity than that of sodium chloride. The oxygen transfer mechanism [24, 33], which is a basic, common and widely accepted mechanism for catalytic gasification, may explain for this result. Specifically, oxygen transfer mechanism is a redox process among coal, gasification agent and catalyst. Take the catalytic process [24, 33] of Na₂CO₃ as an example:

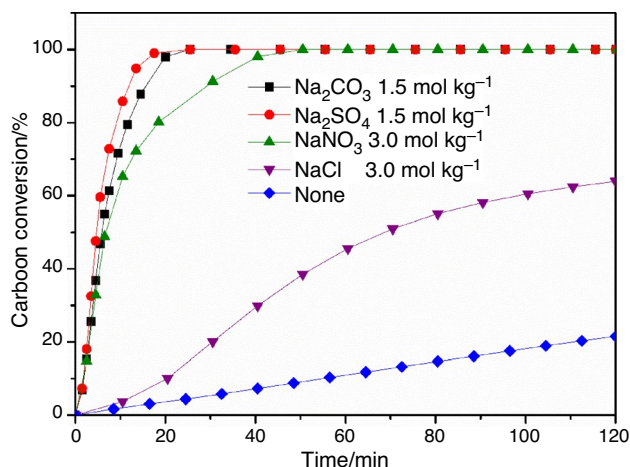
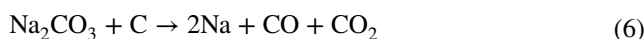
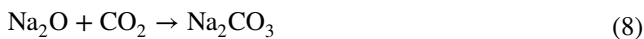


Fig. 2 Carbon conversion of char loaded with different kinds of catalysts at 1173.15 K



where the catalyst is alternately reduced by carbon and oxidized by gaseous reactants, and by this, the oxygen in the gaseous reactant (CO_2 and H_2O) is transferred to the carbon in the coal char. It could be seen that oxide is needed by the catalyst in the oxygen transfer mechanism. In fact, Na_2CO_3 can react with its covered surface carbon and form “surface salt complex.” Some scholars [33] have defined this complex as anionic functional groups, and these groups can weaken the adjacent carbon–carbon bonds, making them susceptible to the attack from the oxidant. Na_2CO_3 , Na_2SO_4 and NaNO_3 are sodium salts that contain oxygen ions, which endow them the ability to supply oxygen to carbon atoms theoretically, while NaCl does not contain oxygen atoms and the catalysis relies on the interactions between NaCl and oxygen atoms in coal, so the catalytic reactivity is relatively poor. As for NaNO_3 , it begins to decompose at 653.15 K; most of the NaNO_3 has decomposed and converted into other Na species before gasification. Thus, oxygen atoms cannot be utilized in catalytic gasification fully and the catalytic activity of it is lower than that of Na_2CO_3 and Na_2SO_4 .

In situ CO_2 gasification of coal char in hot stage microscope

The melting processes of loaded catalysts and the catalytic gasification processes of coal chars would affect the catalytic activity; in order to in situ observe these processes, hot stage microscope was used to capture the pictures during the process of catalytic gasification. The results of char-1.5 Na_2CO_3 are shown in Fig. 3a. It can be seen that the volume (typical area was marked with yellow rectangle) of char-1.5 Na_2CO_3 was shrunk gradually. Simultaneously, the liquid films (typical films were marked with red circle) appeared when the temperature reached 1173.15 K. Then, the liquid films became larger and spread to its neighboring particles. Figure 3b shows the catalytic gasification of char-1.5 Na_2SO_4 , the result is similar to that of char-1.5 Na_2CO_3 except that much more liquid films were observed. Simultaneously, the shrinkage rate (reflects the reaction rate to some extent) of char-1.5 Na_2SO_4 was much faster than that of Na_2CO_3 . In addition, the dynamic video recorded by the hot stage microscope exhibited that the liquid film of Na_2CO_3 and Na_2SO_4 could wet the char particles and spread on the surfaces, and thus facilitated the contact between char particles and catalyst. The pictures of char-3.0 NaNO_3 and char-3.0 NaCl are presented in Fig. 3c and 3d, which also show the similar phenomenon of volume shrinkage but liquid films cannot be captured during the process.

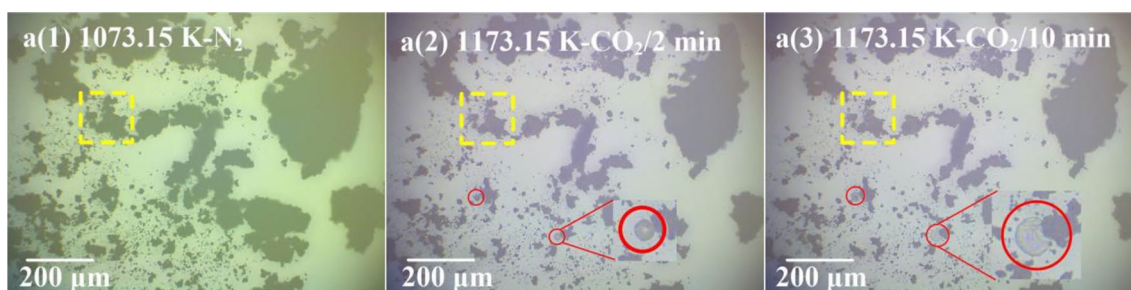
The results of hot stage microscope, visually show that several physical processes have also been involved in the above-mentioned redox process. Firstly, the melting point

of Na_2CO_3 (1124.15 K) and Na_2SO_4 (1157.15 K) is slightly lower than gasification temperature; thus, Na_2CO_3 and Na_2SO_4 become a liquid film just before the beginning temperature of gasification. The liquid Na_2CO_3 and Na_2SO_4 can wet and spread on the exposed surface of char, and finally cover the surface of char. This process can help to obtain a highly dispersed Na_2CO_3 and Na_2SO_4 , while the dispersion process seriously affects the catalytic activity of catalysts. Then, the Na_2CO_3 or Na_2SO_4 can react with its covered surface char, form the above-mentioned “surface salt complex” and play a catalytic role. However, when NaNO_3 or NaCl used as catalyst, liquid films cannot be observed in Fig. 3c and d. Thus, the gasification reactivity of NaNO_3 or NaCl is relatively lower than that of Na_2CO_3 and Na_2SO_4 .

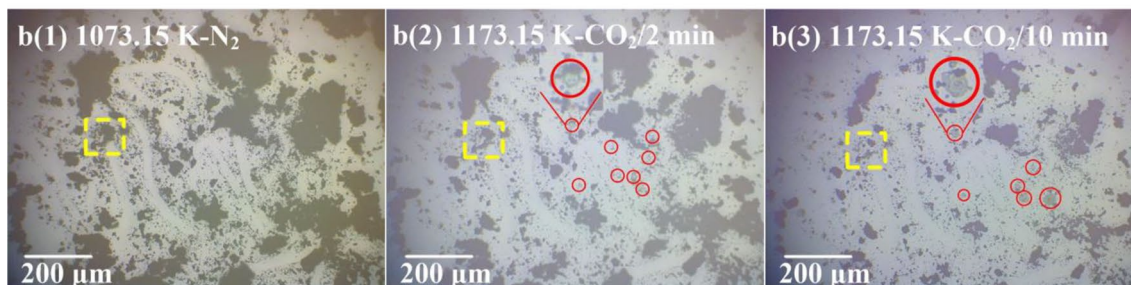
Pore structure and adsorption characteristics of coal char loaded different catalysts

To investigate the effect of catalysts on the surface structure of chars (before the gasification process), specific surface area and pore size distribution of char loaded with different kinds of catalysts were measured by BET. The specific surface areas were calculated from N_2 adsorption data. The results are shown in Fig. 4. It reveals the specific surface area of char-1.5 Na_2SO_4 is much larger than that of other chars. In other words, the addition of Na_2SO_4 can help to create a large amount of surface area in the process of char preparation. The specific surface area of char-1.5 Na_2SO_4 is 8 times larger than that of no catalyst loaded char. The addition of Na_2CO_3 and NaNO_3 have no obvious effect on the increase in the surface area. The specific surface area of char-1.5 Na_2CO_3 and raw char is basically the same. In addition, the specific surface area of char-3.0 NaNO_3 is increased compared with raw char, but the amount of it is very small.

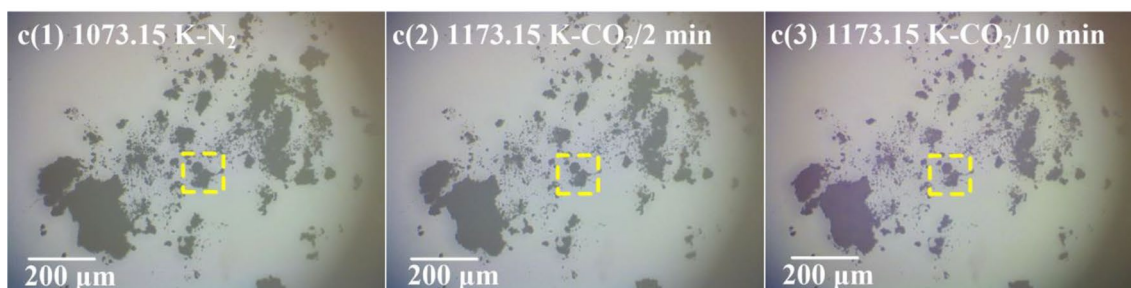
The pore size distributions are presented in Fig. 5. It can be found that the most probable pore radius of chars loaded catalyst is all larger than that of raw char, among which char-1.5 NaNO_3 has the largest pore size and that may be due to the decomposition of NaNO_3 . At lower temperature (below 973.15 K), NaNO_3 is decomposed and released O_2 , N_2 , NO , etc. from the pore of coal. The movement of these gas molecules may increase the aperture of pores. As for char-1.5 Na_2SO_4 and char-1.5 Na_2CO_3 , the most probable pore radius of both are located at 6.5 nm. The difference between them is that the pore distribution of the former is relatively broad around 6.5 nm and it has some micropore around 2 nm. Moreover, which indicates that Na_2SO_4 create a large number of micropores in the process of char preparation [34]. These micropores and mesoporous structures endow the char-1.5 Na_2SO_4 with the largest specific surface area. The pore size distribution of char- NaCl and char is almost same except that the most probable pore radius of char- NaCl is 5.5 nm while that of char is 5 nm.



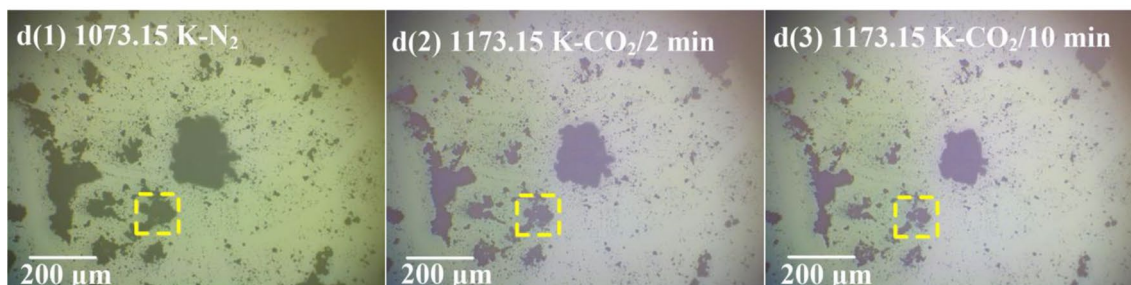
a. Morphology variation of char-1.5 Na_2CO_3 in the process of gasification



b. Morphology variation of char-1.5 Na_2SO_4 in the process of gasification



c. Morphology variation of char-3.0 NaNO_3 in the process of gasification



d. Morphology variation of char-3.0 NaCl in the process of gasification

Fig. 3 a Morphology variation of char-1.5 Na_2CO_3 in the process of gasification. b Morphology variation of char-1.5 Na_2SO_4 in the process of gasification. c Morphology variation of char-3.0 NaNO_3 in the

process of gasification. d Morphology variation of char-3.0 NaCl in the process of gasification

Figure 6 shows the SEM images of char which loaded with different kinds of catalysts. There are many large pores

(the diameter is about 200 nm) on the surface of char-1.5 Na_2SO_4 . In other images, no obvious pores can be observed.

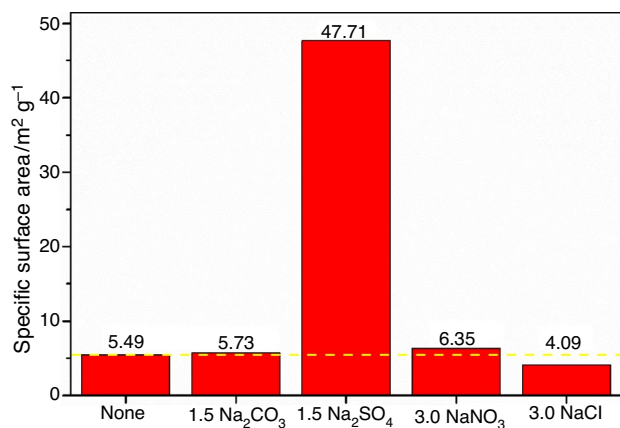


Fig. 4 Specific surface area of char loaded with different kinds of catalysts

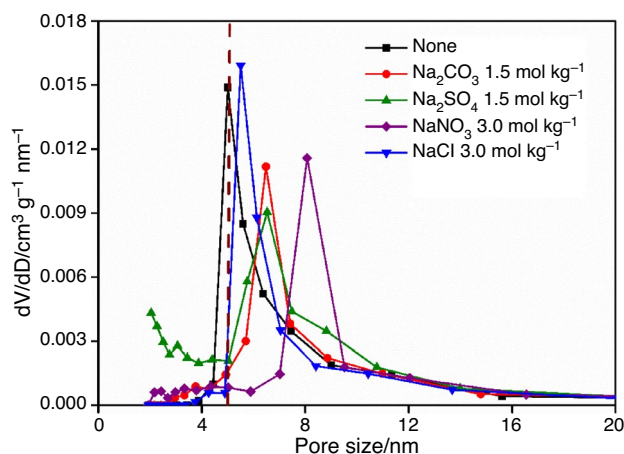


Fig. 5 Pore size distribution of char loaded with different kinds of catalysts

Hence, it can be deduced that the appearance of many large pores on the surface of char is due to the addition of Na₂SO₄. However, limited by the accuracy of SEM, micropores and mesopores are difficult to be observed and direct evidence about the result of BET cannot be provided. Even so, the appearance of macropores increases the specific surface area of coal char, which provides conditions for increasing CO₂ adsorption and the reaction rate.

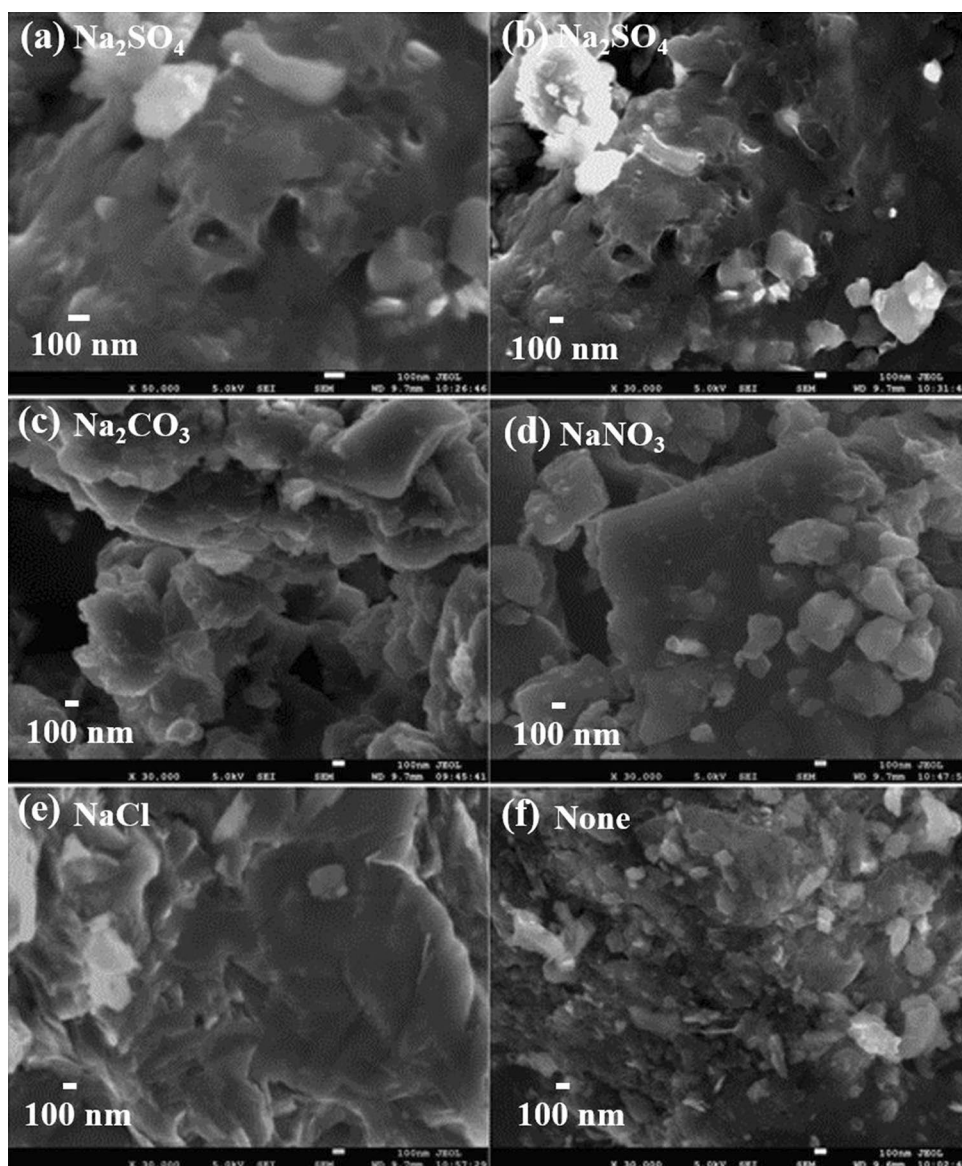
The active site which is directly related to the gasification reactivity of char is usually measured by chemical adsorption of CO₂ [35]. Figure 7a describes the process of CO₂ adsorption (char-1.5 Na₂SO₄ as an example) and desorption. Figure 7b shows the CO₂ adsorption quantity of char loaded with different kinds of catalysts, which is used as a parameter to reflect the gasification reactivity, where the weak adsorption process is a kind of reversible adsorption and belongs to the physical adsorption. The difference of weak

adsorption capacity among these samples is not significant and the larger specific surface area corresponds to the larger capacity of weak adsorption, among which the largest specific surface area is char loaded with 1.5 mol kg⁻¹ Na₂SO₄ and the weak adsorption quantity of it is also the largest. The strong adsorption belongs to the chemical adsorption and corresponds closely with the catalytic reactivity. The quantity of it among chars loaded with different kinds of catalysts is different. The order of strong adsorption quantity is as follows: char-1.5 Na₂SO₄ > char-1.5 Na₂CO₃ > char-3.0 NaNO₃ > char-3.0 NaCl > char. This sequence is consistent with the order of catalytic reactivity. It clearly indicates that the chemical adsorption quantity of char catalyst to CO₂ influence the reactivity of gasification directly. The strong adsorption quantity of char-1.5 Na₂SO₄ and char-1.5 Na₂CO₃ is relatively larger, while the adsorption capacity of char-1.5 Na₂SO₄ is higher than that of char-1.5 Na₂CO₃ slightly. These are in accordance with the results of gasification process, where the catalytic reactivity of Na₂SO₄ and Na₂CO₃ is relatively high while the catalytic reactivity of Na₂SO₄ is slightly higher than that of Na₂CO₃. That is probably because the addition of Na₂SO₄ can increase micropores and active sites in the process of char preparation. Thus, the addition of sodium salt catalysts enhanced the CO₂ adsorption ability of char and improved its gasification reactivity.

Catalytic gasification reactivity of char-Na₂CO₃ and char-Na₂SO₄

The catalytic activity of Na₂CO₃ and Na₂SO₄ are relatively high; in order to explore suitable catalytic gasification temperature, char-1.5 Na₂CO₃ and char-1.5 Na₂SO₄ were gasified at 1123.15 K, 1173.15 K and 1223.15 K, respectively. The carbon conversion of char-1.5 Na₂CO₃ and char-1.5 Na₂SO₄ is shown in Fig. 8. It can be seen that the carbon conversion rate of char-1.5 Na₂CO₃ and char-1.5 Na₂SO₄ at 1123.15 K is relatively slow especially near the end of reaction. The difference of carbon conversion rate at 1173.15 K and 1223.15 K is not obvious. To clearly compare the effect of temperature and determine the appropriate temperature, $\tau_{0.5}$ and reaction time were selected as evaluation parameters. The faster the reaction, the smaller the value of $\tau_{0.5}$ will be. Table 3 shows that when the temperature rises from 1123.15 to 1173.15 K, the $\tau_{0.5}$ of char-1.5 Na₂CO₃ reduces quickly from 8.4 to 5.8 min. Reaction time of char-1.5 Na₂CO₃ reduces nearly the half (from 45 to 25 min). Similar to char-1.5 Na₂CO₃, $\tau_{0.5}$ of char-1.5 Na₂SO₄ also reduces from 6.0 to 4.8 min. When the temperature further reaches 1223.15 K, the changes of these parameters are not as significant as before. $\tau_{0.5}$ of char-1.5 Na₂CO₃ changes from 5.8 to 4.8 min, and for char-1.5 Na₂CO₃, it changes from 4.8 to 3.8 min. Considering the influence of temperature on

Fig. 6 SEM images of char loaded with different kinds of catalysts



reaction speed and ash residue, 1173.15 K is regarded as an appropriate catalytic gasification temperature.

To further compare the catalytic activity of Na_2CO_3 and Na_2SO_4 in coal gasification, coal chars with various Na_2CO_3 and Na_2SO_4 additions were gasified at 1173.15 K. The curves of carbon conversion versus gasification time are shown in Figs. 9 and 10. It can be seen that the reaction rate improved with the increasing addition of Na_2CO_3 and Na_2SO_4 . Fortunately, the carbon conversion can reach 100% within a few minutes when enough Na_2CO_3 or Na_2SO_4 was used. When the addition of Na_2CO_3 is below 1.5 mol kg^{-1} or Na_2SO_4 is below 1.0 mol kg^{-1} , the reaction rate is relatively low and the carbon conversion cannot reach balance even reaction last 120 min; however, when the addition of Na_2CO_3 exceed 1.5 mol kg^{-1} or Na_2SO_4 exceed 1.0 mol kg^{-1} , the time required to achieve

carbon conversion balance is not clearly reduced with the increasing addition of catalysts. That is to say, the gasification rate is no longer accelerated with the increasing addition of Na_2CO_3 or Na_2SO_4 , and thus, 1.5 mol kg^{-1} and 1.0 mol kg^{-1} are the saturation addition of them, respectively.

In order to intuitively compare the catalytic activity of Na_2CO_3 and Na_2SO_4 , $R_{0.5}$ was introduced. When the gasification rate becomes faster or the reaction between coal and catalyst becomes stronger, the value of $R_{0.5}$ will be larger. The $R_{0.5}$ of coal char loaded with various Na_2CO_3 and Na_2SO_4 additions is shown in Table 4. It can be seen that $R_{0.5}$ of Na_2SO_4 is always larger than that of Na_2CO_3 , i.e., the gasification rate of Na_2SO_4 is faster than that of Na_2CO_3 . The trends of $R_{0.5}$ in Fig. 11 more clearly show that catalytic activity of Na_2SO_4 is better especially when the addition of

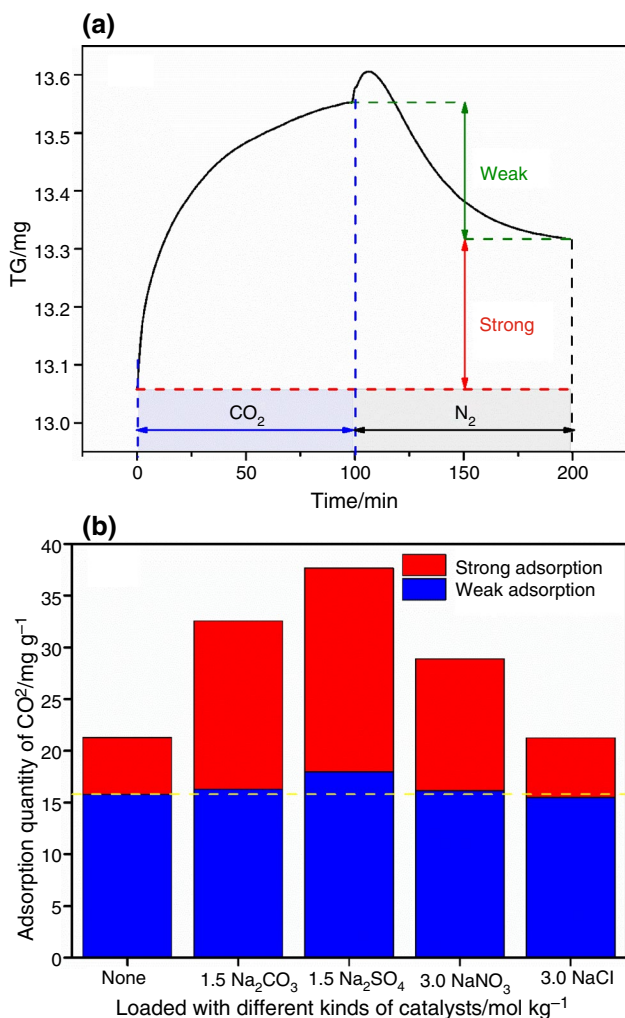


Fig. 7 a Process of CO₂ adsorption and desorption, b CO₂ adsorption quantity of char loaded with different kinds of catalysts

catalyst is 1.0 mol kg⁻¹. Both of Na₂SO₄ and Na₂CO₃ are oxygen-containing sodium salts, but catalytic reactivity of the former is better, which aroused our attention.

In order to compare the effect of catalyst on kinetics, a modified random pore model (MRPM) was adopted. The MRPM [6] was indicated as below:

$$\frac{dx}{dt} = k_{MRPM}(1 - x_i)\sqrt{1 - \psi \ln(1 - x)}[1 + (c - cx)^p] \quad (9)$$

where the *c* presents the dimensionless constant and *p* presents the dimension power law constant. Ψ is a dimensionless structural parameter indicating the pore structure. k_{MRPM} is the reaction rate constant of the MRPM model. By fitting the experimental results with the MRPM, it can be observed that all samples can be well fitted. The curve fitted of samples gasified at 1223.15 K was shown in Fig. 12.

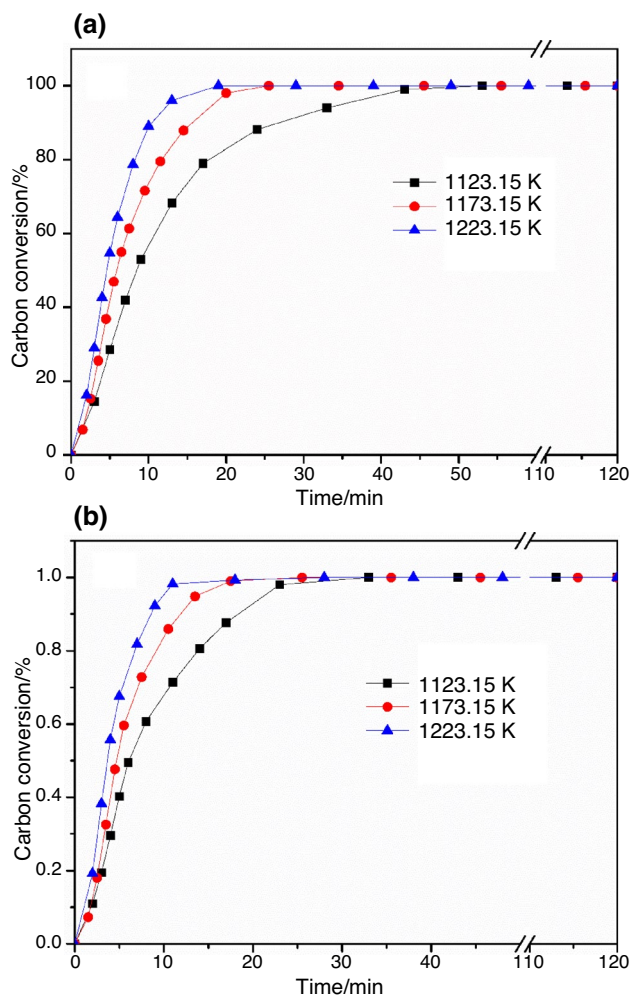


Fig. 8 Carbon conversion of char loaded with 1.5 mol catalyst at different temperatures a char-1.5 Na₂CO₃, b char-1.5 Na₂SO₄

Table 3 $\tau_{0.5}$ and reaction time of char-1.5 Na₂CO₃ and char-1.5 Na₂SO₄ at different temperatures

Catalyst	Addition/mol kg ⁻¹	Temperature/K	$\tau_{0.5}$ /min	Reaction time/min
Na ₂ CO ₃	1.5	1123.15	8.4	45.0
Na ₂ CO ₃	1.5	1173.15	5.8	25.0
Na ₂ CO ₃	1.5	1223.15	4.8	15.0
Na ₂ SO ₄	1.5	1123.15	6.0	33.0
Na ₂ SO ₄	1.5	1173.15	4.8	17.5
Na ₂ SO ₄	1.5	1223.15	3.8	11.0

Assuming the concentration of CO₂ was kept constant in the gasification process, the activation energy could be calculated by the Arrhenius law in Eq. 7.

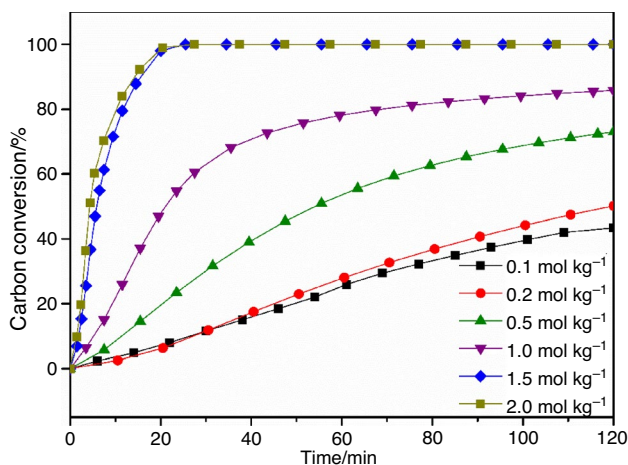


Fig. 9 Carbon conversion of char with various Na_2CO_3 additions at 1173.15 K

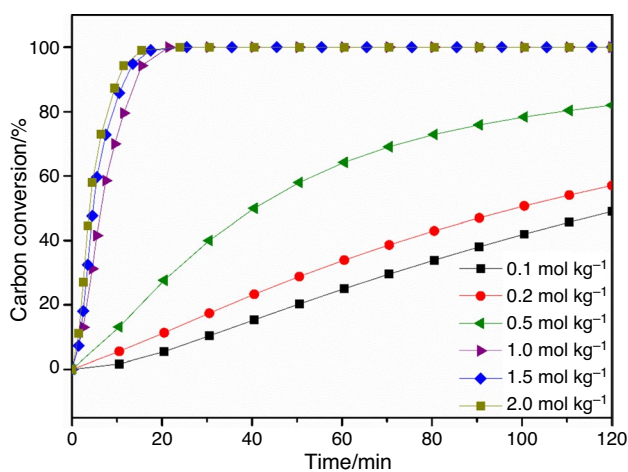


Fig. 10 Carbon conversion of char with various Na_2SO_4 additions at 1173.15 K

Table 4 Changes of $R_{0.5}$ with various catalysts additions at 1173.15 K

Addition/mol kg^{-1}	Na_2CO_3 $R_{0.5}/\text{min}^{-1}$	Na_2SO_4 $R_{0.5}/\text{min}^{-1}$
0.2	0.0042	0.0050
0.5	0.0090	0.0124
1.0	0.0238	0.0714
1.5	0.0833	0.0962
2.0	0.1163	0.1250

$$k = A \exp\left(-\frac{E_a}{RT}\right) \quad (10)$$

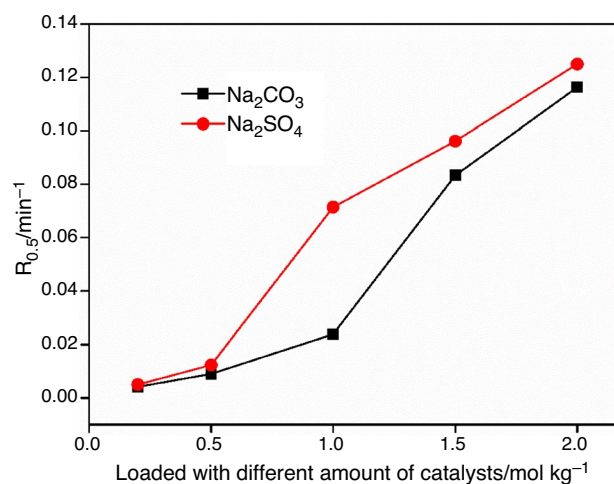


Fig. 11 Changes of $R_{0.5}$ with various catalysts additions

where A is pre-exponential factor (min^{-1}), R is the universal gas constant ($\text{J mol}^{-1} \text{K}^{-1}$) and E_a is the activation energy (kJ mol^{-1}). The activation energy and pre-exponential factor of different samples could be calculated from the slope and intercept of the $\ln k$ vs $1/T$ (Fig. 11b).

The fitting parameters results of 1123.15 K, 1173.15 K and 1223.15 K applied MPAM and the correlation coefficients (R^2) are summarized in Table 5. It can be seen that the reaction rate constant (k) increased with the temperature for both samples and the results were consistent with the results of $\tau_{0.5}$. The E_a value of char-1.5 Na_2SO_4 is lower than that of char-1.5 Na_2CO_3 . It can be deduced that the addition of Na_2SO_4 reduces activation energy more significantly than that of char-1.5 Na_2CO_3 . This result can explain the $R_{0.5}$ of char- Na_2SO_4 always larger than that of char- Na_2CO_3 (in Fig. 10) to some extent. In addition, the ψ value of char-1.5 Na_2SO_4 is significantly smaller than that of char-1.5 Na_2CO_3 . It can be deduced that pore structure of char-1.5 Na_2CO_3 and char-1.5 Na_2SO_4 is different, even though the specific differences cannot be defined.

Figure 13a shows the XRD spectra of catalytic gasification ash with various Na_2CO_3 additions at 1173.15 K. When the dosage of Na_2CO_3 is less than 0.2 mol kg^{-1} , the main mineral in ash is quartz. With the increasing addition of Na_2CO_3 , $\text{NaAlSi}_3\text{O}_8$ (nepheline) appears and the characteristic peak intensity of it increases gradually. When the addition of Na_2CO_3 up to 1.5 mol kg^{-1} , some characteristic peaks of $\text{Na}_7\text{Al}_6\text{Si}_6\text{O}_{24}\text{S}_3$ (lazurite) appear. It can be inferred that when the addition of Na_2CO_3 is not enough, the main form of SiO_2 is quartz. With the increasing of Na_2CO_3 , minerals in ash (Al_2O_3 , SiO_2 etc.) reacted with added Na_2CO_3 and complex compound such as $\text{NaAlSi}_3\text{O}_8$, $\text{Na}_7\text{Al}_6\text{Si}_6\text{O}_{24}\text{S}_3$ was formed.

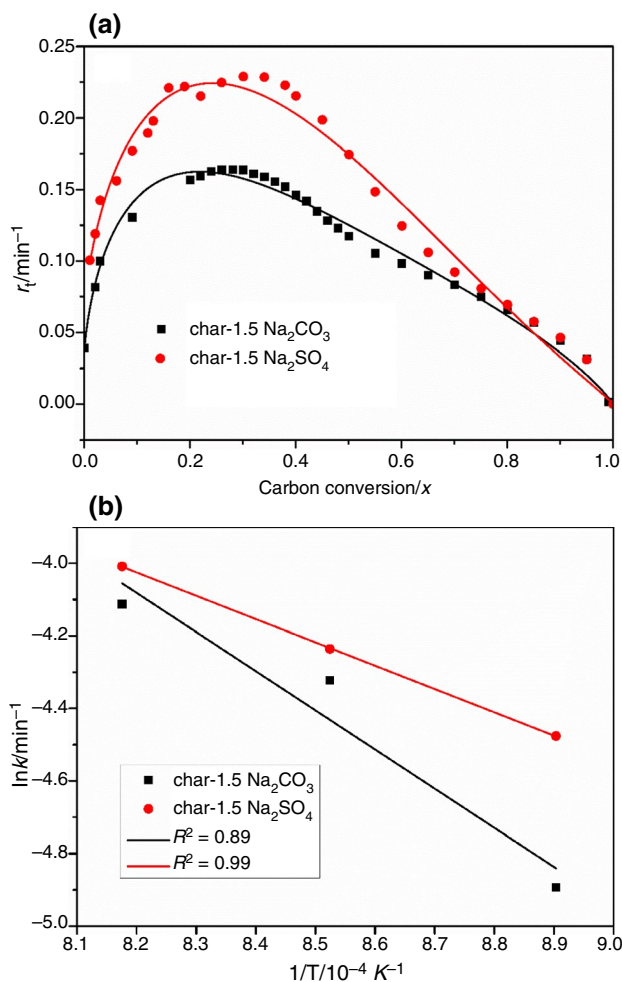


Fig. 12 a Application of MRPM to fit the gasification rate of samples at 1223.15 K; b Arrhenius plot of different samples

Figure 14a shows the XRD spectra of catalytic gasification ash with various Na₂SO₄ additions at 1173.15 K. Similar to the law of mineral transformation above, the

mineral forms of catalytic gasification ash loaded with Na₂SO₄ also changed from SiO₂(quartz) to NaAlSiO₄ (albite, nepheline) and then Na₇Al₆Si₆O₂₄S₃ (lazurite). However, the spectra of Na₂CO₃, Na₂O does not appear in both spectra. It can be inferred that the highly mobile sodium in the gasification process can easily react with minerals in coal to form deactivated matters. This conclusion is consistent with our team’s previous results “When the addition of catalysts is relatively low, sodium salts react with minerals and cannot give full play to its catalytic capability” [29]. With the increasing addition of sodium salts, the amount of catalyst that participating in the catalytic reaction increases and thus the rate of catalytic gasification can also be accelerated. It is noteworthy that when the addition of Na₂CO₃ or Na₂SO₄ up to 1.5 mol kg⁻¹, the minerals in ash are NaAlSiO₄ (nepheline) and Na₇Al₆Si₆O₂₄S₃ (lazurite). Our previous study has shown that these minerals are easily dissolved in acid solutions [16]. It indicates that when the catalyst dosage is appropriate, not only the catalytic effect is good, but also the catalysts can be recycled and reused.

In order to figure out the change of mineral content with various catalysts additions, thermodynamic equilibrium calculation with FactSage was used. The results of it are shown in Figs. 13b and 14b. When the addition of Na₂CO₃ less than 0.5 mol kg⁻¹, the content of SiO₂ (quartz) and Al₆Si₂O₁₃ (mullite) decreased gradually; simultaneously, the content of NaAlSi₃O₈ (albite) and NaAlSiO₄ (nepheline) increased gradually. With the increasing addition of Na₂CO₃, NaAlSi₃O₈ (albite) disappears gradually and the content of NaAlSiO₄ (nepheline) increased first and then decreased. It indicates that when the addition of Na₂CO₃ is insufficient, part of quartz and mullite transform into albite. When the addition of Na₂CO₃ is enough, albite transforms into nepheline. With the increasing addition of Na₂CO₃, some slag will appear and the content of nepheline will be decreased. Similarly,

Table 5 Kinetic parameters and regression coefficients of the samples

Sample	T(K)	k/min ⁻¹	ψ	c	p	R ²	Ea/kJ·mol ⁻¹	A/min ⁻¹
char-1.5 Na ₂ CO ₃	1123.15	0.00750	255.947	1.037	2.763	0.982	89.683	125.211
	1173.15	0.01327	180.274	1.206	2.129	0.981		
	1223.15	0.01637	205.796	1.139	2.279	0.983		
char-1.5 Na ₂ SO ₄	1123.15	0.01138	80.9221	4.625	0.936	0.978	53.369	3.450
	1173.15	0.01447	94.620	3.994	0.851	0.973		
	1223.15	0.01816	89.462	2.786	1.060	0.977		

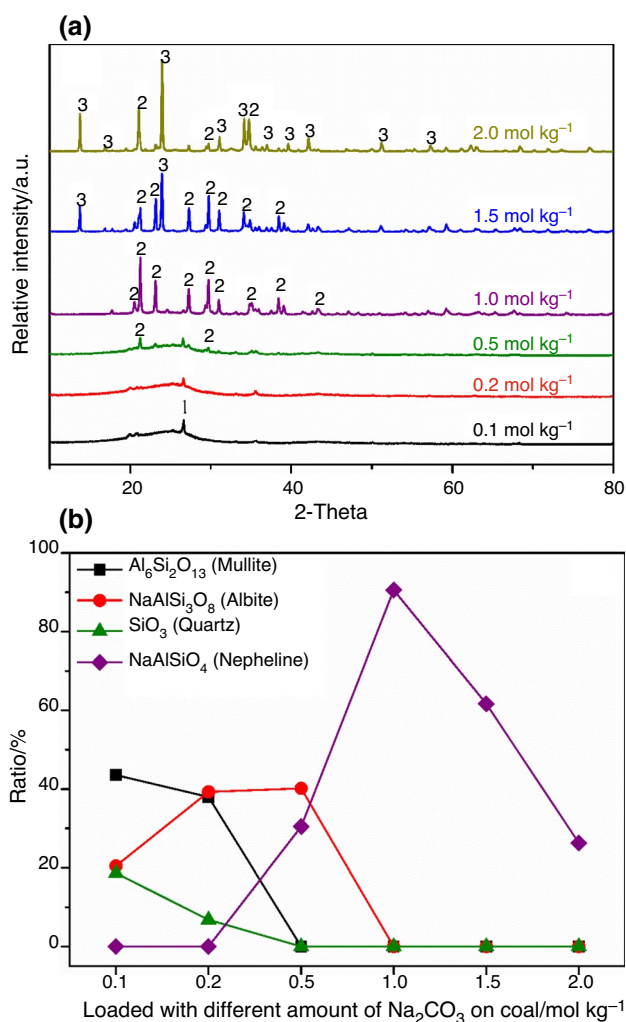


Fig. 13 Mineral transformation of catalytic gasification ash with various Na_2CO_3 additions at 1173.15 K **a** XRD spectra (1) SiO_2 quartz; (2) NaAlSiO_4 nepheline; (3) $\text{Na}_7\text{Al}_6\text{Si}_6\text{O}_{24}\text{S}_3$ lazurite, **b** FactSage simulation

when Na_2SO_4 as catalyst, the transformations of minerals are basically the same.

Conclusions

Catalytic gasification reactivity of sodium salts was investigated by TGA, BET, hot stage microscope, XRD and thermodynamic equilibrium calculations. The results indicate that catalytic reactivity of sodium salts is as follows: $\text{Na}_2\text{SO}_4 > \text{Na}_2\text{CO}_3 > \text{NaNO}_3 > \text{NaCl}$ when the addition of catalysts based on per unit of coal correspond to a certain mole of Na^+ in solution. With the help of catalyst, char catalyst has more specific surface area than raw char in the char preparation, especially char- Na_2SO_4 . That endows char catalyst with stronger chemisorption of CO_2 and more active

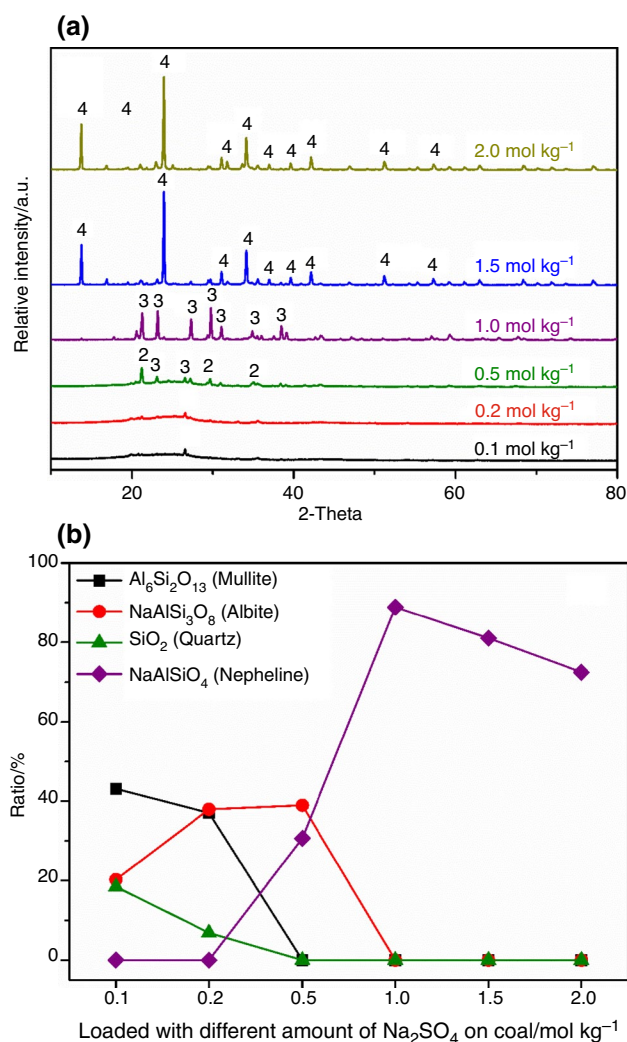


Fig. 14 Mineral transformation of catalytic gasification ash with various Na_2SO_4 additions at 1173.15 K **a** XRD spectra (1) SiO_2 quartz; (2) NaAlSiO_4 nepheline; (3) NaAlSiO_4 albite; (4) $\text{Na}_7\text{Al}_6\text{Si}_6\text{O}_{24}\text{S}_3$ lazurite, **b** FactSage simulation

sites. In the gasification process, Na_2SO_4 and Na_2CO_3 melt and become liquid film wet the carbon and spread over its expose surfaces, facilitate the contact between carbon and catalyst and accelerate the gasification reaction.

Acknowledgements The work is financially supported by the National Science Foundation of China (21676289), the Natural Science Fund of Shanxi Province (201801D221091), the research supported by the Chinese Academy of Sciences (CAS)/State Administration of Foreign Experts Affairs (SAFEA) International Partnership Program for Creative Research Teams and Youth Innovation Promotion Association (2014156).

Funding The authors declare no competing financial interest.

References

- Minchener AJ. Coal gasification for advanced power generation. *Fuel*. 2005;84:2222–35.
- May A, Salvadó J, Torras C, Montané D. Catalytic gasification of glycerol in supercritical water. *Chem Eng J*. 2010;160:751–9.
- Jahirul M, de Lasa HI. Catalytic steam gasification of biomass surrogates: thermodynamics and effect of operating conditions. *Chem Eng J*. 2016;293:232–42.
- Arena U. Process and technological aspects of municipal solid waste gasification. A review. *Waste Manag*. 2012;32:625–39.
- Luo S, Xiao B, Hu Z, Liu S. Effect of particle size on pyrolysis of single-component municipal solid waste in fixed bed reactor. *Int J Hydrogen Energy*. 2010;35:93–7.
- Irfan MF, Usman MR, Kusakabe K. Coal gasification in CO₂ atmosphere and its kinetics since 1948: a brief review. *Energy*. 2011;36:12–40.
- And XY, Leung DYC, Jie C, Wang J, Fu Y, Wu C. Characteristics of the synthesis of methanol using biomass-derived syngas. *Energy Fuels*. 2005;19:305–10.
- Luu MT, Milani D, Wake M, Abbas A. Analysis of di-methyl ether production routes: process performance evaluations at various syngas compositions. *Chem Eng Sci*. 2016;149:143–55.
- Pereira EG, da Silva JN, de Oliveira JL, Machado CS. Sustainable energy: A review of gasification technologies. *Renew Sustain Energy Rev*. 2012;16:4753–62.
- Wei J, Gong Y, Ding L, Yu J, Yu G. Influence of biomass ash additive on reactivity characteristics and structure evolution of coal char–CO₂ gasification. *Energy Fuels*. 2018;32:10428–36.
- Li N, Li Y, Ban Y, Song Y, Zhi K, Teng Y, He R, Zhou H, Liu Q, Qi Y. Direct production of high hydrogen syngas by steam gasification of Shengli lignite/chars: remarkable promotion effect of inherent minerals and pyrolysis temperature. *Int J Hydrogen Energy*. 2017;42:5865–72.
- Lu R, Wang J, Liu Q, Wang Y, Te G, Ban Y, Li N, Zhang X, He R, Zhou H, Zhi K. Catalytic effect of sodium components on the microstructure and steam gasification of demineralized Shengli lignite char. *Int J Hydrogen Energy*. 2017;42:9679–87.
- Yuan X, Fan S, Zhao L, Kim H-T. Investigations of both catalytic steam gasification of Indonesian lanna coal and potassium catalyst recovery using K₂CO₃ as a catalyst. *Energy Fuels*. 2016;30:2492–502.
- Liu Y, Guan Y-J, Guan Y. Na₂CO₃ catalyzed CO₂ gasification of coal char and its intermediate complexes. *Res Chem Intermed*. 2018;44:7789–803.
- Bai Y, Zhu S, Luo K, Gao M, Yan L, Li F. Coal char gasification in H₂O/CO₂: Release of alkali and alkaline earth metallic species and their effects on reactivity. *Appl Therm Eng*. 2017;112:156–63.
- Li L, Wang Z, Huang J, Ji S, Mei Y, Wang Y, Fang Y. Comparison of silica leaching behaviors from the acid-leached residue of catalytic gasification and combustion. *Energy Fuels*. 2017;31:10745–51.
- Liu Y, Guan Y, Zhang K. CO₂ gasification performance and alkali/alkaline earth metals catalytic mechanism of Zhundong coal char. *Korean J Chem Eng*. 2018;35:859–66.
- Li Y, Zhou C, Li N, Zhi K, Song Y, He R, Teng Y, Liu Q. Production of high H₂/CO syngas by steam gasification of shengli lignite: catalytic effect of inherent minerals. *Energy Fuels*. 2015;29:4738–46.
- Yuan X, Fan S, Choi SW, Kim H-T, Lee KB. Potassium catalyst recovery process and performance evaluation of the recovered catalyst in the K₂CO₃-catalyzed steam gasification system. *Appl Energy*. 2017;195:850–60.
- Courson C, Udron L, Swierczynski D, Petit C, Kiennemann A. Hydrogen production from biomass gasification on nickel catalysts-Tests for dry reforming of methane. *Catal Today*. 2002;76:75–86.
- Zhang F, Xu D, Wang Y, Argyle MD, Fan M. CO₂ gasification of Powder River Basin coal catalyzed by a cost-effective and environmentally friendly iron catalyst. *Appl Energy*. 2015;145:295–305.
- Ding L, Dai Z, Wei J, Zhou Z, Yu G. Catalytic effects of alkali carbonates on coal char gasification. *J Energy Inst*. 2017;90:588–601.
- Ding L, Zhou Z, Guo Q, Huo W, Yu G. Catalytic effects of Na₂CO₃ additive on coal pyrolysis and gasification. *Fuel*. 2015;142:134–44.
- Wu X, Wang J. K₂CO₃-catalyzed steam gasification of ash-free coal char in a pressurized and vertically blown reactor. Influence of pressure on gasification rate and gas composition. *Fuel Process Technol*. 2017;159:9–18.
- Karimi A, Semagina N, Gray MR. Kinetics of catalytic steam gasification of bitumen coke. *Fuel*. 2011;90:1285–91.
- Kopyscinski J, Lam J, Mims CA, Hill JM. K₂CO₃ catalyzed steam gasification of ash-free coal. Studying the effect of temperature on carbon conversion and gas production rate using a drop-down reactor. *Fuel*. 2014;128:210–9.
- Zhang F, Xu D, Wang Y, Wang Y, Gao Y, Popa T, Fan M. Catalytic CO₂ gasification of a powder river basin coal. *Fuel Process Technol*. 2015;130:107–16.
- Wang Y, Wang Z, Huang J, Fang Y. Catalytic gasification activity of Na₂CO₃ and comparison with K₂CO₃ for a high-aluminum coal char. *Energy Fuels*. 2015;29:6988–98.
- Mei Y, Wang Z, Fang H, Wang Y, Huang J, Fang Y. Na-containing mineral transformation behaviors during Na₂CO₃-catalyzed CO₂ gasification of high-alumina coal. *Energy Fuels*. 2017;31:1235–42.
- Yang Y, Lin X, Chen X, Guo W, Wang Y, Zhang J, Kawa O. Investigation on the effects of different forms of sodium, chlorine and sulphur and various pretreatment methods on the deposition characteristics of Na species during pyrolysis of a Na-rich coal. *Fuel*. 2018;234:872–85.
- Li J, Zhu M, Zhang Z, Zhang K, Shen G, Zhang D. The mineralogy, morphology and sintering characteristics of ash deposits on a probe at different temperatures during combustion of blends of Zhundong lignite and a bituminous coal in a drop tube furnace. *Fuel Process Technol*. 2016;149:176–86.
- Mei Y, Wang Z, Bai J, He C, Li W, Liu T, Huang J, Fang Y. Mechanism of Ca additive acting as a deterrent to Na₂CO₃ deactivation during catalytic coal gasification. *Energy Fuels*. 2019;33:938–45.
- Wood B, Sancier K. The mechanism of the catalytic gasification of coal char: a critical review. *Catal Rev Sci Eng*. 1984;26:233–79.
- Guo S, Jiang Y, Liu T, Zhao J, Huang J, Fang Y. Investigations on interactions between sodium species and coal char by thermogravimetric analysis. *Fuel*. 2018;214:561–8.
- Xu K, Hu S, Su S, Xu C, Sun L, Shuai C, Jiang L, Xiang J. Study on char surface active sites and their relationship to gasification reactivity. *Energy Fuels*. 2013;27:118–25.

Publisher's Note Springer Nature remains neutral with regard to jurisdictional claims in published maps and institutional affiliations.